

Performance Analysis of Hybrid Cellular and Cell-free MIMO Network

Zhuoyin Dai*, Jingran Xu*, Xiaoli Xu*, Ruoguang Li* and Yong Zeng*†

*National Mobile Communications Research Laboratory, Southeast University, Nanjing 210096, China

†Purple Mountain Laboratories, Nanjing 211111, China

Email: {zhuoyin_dai, jingran_xu, xiaolixu, ruoguangli, yong_zeng}@seu.edu.cn

Abstract—Cell-free wireless communication is envisioned as one of the most promising network architectures, which can achieve stable and uniform communication performance while improving the system energy and spectrum efficiency. The deployment of cell-free networks is envisioned to be a long-term evolutionary process, in which cell-free access points (APs) will be gradually introduced into the communication network and collaborate with the existing cellular base stations (BSs). To further explore the performance limits of hybrid cellular and cell-free networks, this paper develops a hybrid network model based on stochastic geometric toolkits, which reveals the coupling of the signal and interference from both the cellular and cell-free networks. Specifically, the conjugate beamforming is applied in hybrid cellular and cell-free networks, which enables user equipment (UE) to benefit from both cellular BSs and cell-free APs. The aggregate signal received from the hybrid network is approximated via moment matching, and coverage probability is characterized by deriving the Laplace transform of the interference. The analysis of signal strength and coverage probability is verified by extensive simulations.

I. INTRODUCTION

The future wireless communication networks will witness a proliferation of mobile applications and unprecedented growth in wireless data. The realization of higher spectrum and energy efficiency with superior costs remains a challenging issue in current research. As one of the most prominent wireless technologies proposed in recent years, cell-free network is considered as a promising network architecture in the beyond fifth-generation (B5G) and sixth generation (6G) mobile communication system [1]. Different from traditional cellular systems, cell-free network is a user-centric coverage architecture that discards the traditional concept of cellular boundaries [2]. The central processing unit (CPU) controls the access points (APs) to cooperate to provide services to user equipment (UE) on the same time-frequency resources, thus realizing higher spatial multiplexing [3], [4]. Cell-free network improves the energy and spectral efficiency of the system, and effectively reduces the performance gaps between UE by ensuring that there are spatially short-range APs that provide stable services to UE.

However, the deployment of cell-free systems in existing commercial mobile networks still faces serious challenges. First, the construction of cell-free systems requires the deployment of the distributed APs throughout the network and the construction of the corresponding fronthaul links, which brings heavy time costs and deployment expenses. Second,

simply introducing the cell-free system without cooperation will inevitably cause mutual interference with existing cellular systems, significantly limiting the system performance. Therefore, the deployment of cell-free systems is bound to be a long-term evolutionary process, and hybrid cellular and cell-free cooperation networks are both a necessity and a desirable choice for B5G and 6G.

Some recent works have investigated the performance analysis and resource allocation of hybrid cellular and cell-free networks. A cell-free and legacy cellular coexistence system deployed on the existing system architecture, as well as the corresponding precoding, power control, etc., are outlined in [5]. With appropriate UE association criteria and coordinated beamforming, hybrid cell-free and small cell systems can provide superior downlink rates for static and dynamic UE than the single architecture [6]. However, the above works do not take into account the impact of the spatial distribution of base stations (BSs), APs, and UE on network performance.

Due to the densification and irregularity of wireless node distributions in the network, traditional grid-based deployment models are difficult to reflect the practical system performance. Stochastic geometry models the spatial distribution of wireless nodes with point processes and can effectively characterize the lower bound of the actual system performance. There have been some works using stochastic geometry to analyze the performance of cell-free networks and coordinated multiple points (CoMP) communication in terms of energy efficiency (EE) [7], power control [8] and channel hardening analysis [9], etc. However, there is still a lack of work related to the characterization of hybrid cellular and cell-free networks. In addition, the existing stochastic geometry-based heterogeneous network studies, which separate different network layers from each other [10], are not applicable to the analysis of hybrid cellular and cell-free networks.

To gain some insights of the performance limit of the hybrid network, this paper develops a stochastic geometry-based model for hybrid cellular and cell-free networks, which reveals the coupling of the signal and interference from both the cellular and cell-free networks. However, the aggregate signals from the BSs and APs with conjugate beamforming make it difficult to characterize the distribution of the signal strength and the corresponding signal-to-interference plus noise ratio (SINR). To tackle this issue, we first derive the closed-form expressions for the average signal strength and

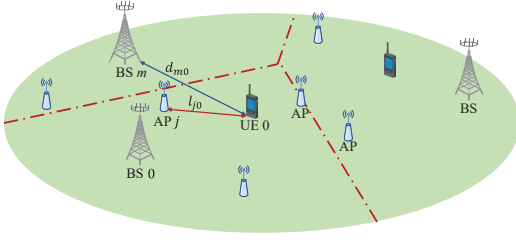


Fig. 1. Hybrid cellular and cell-free network.

interference power from the APs, and then the aggregate signal strength distribution is approximated via moment matching. Finally, the coverage probability is characterized on the basis of the Laplace transform of the system interference power. The analysis of network coverage probability is verified by extensive simulations, and it can be used to guide the network deployment and interference management in the hybrid cellular and cell-free networks.

II. SYSTEM MODEL

As shown in Fig. 1, a hybrid cellular and cell-free network is considered in this paper. The locations of BSs, cell-free APs, and single-antenna UE are modeled by independent homogeneous Poisson point processes (HPPP) Λ_B , Λ_A and Λ_U , with density λ_B/km^2 , λ_A/km^2 and λ_U/km^2 , respectively. Each BS is equipped with N_B antennas, while each AP is equipped with N_A antennas. Considering the different configurations that AP and BS can support, P_A and P_B denote the maximum downlink power of AP and BS with $P_A < P_B$. In the network, d_{mi} and l_{ji} denote the distance between BS m and UE i , and that between AP j and UE i , respectively. We consider a typical UE, referred as UE 0, which is jointly served by the closest BS, named BS 0, with the distance d_{00} , and all the cell-free APs in \mathcal{A} . The channel vector between BS m and UE i is denoted by $\mathbf{h}_{mi} \triangleq [h_{mi,1}, \dots, h_{mi,N_B}] \in \mathbb{C}^{N_B \times 1}$, while the channel vector between AP j and UE i is $\mathbf{g}_{ji} \triangleq [g_{ji,1}, \dots, g_{ji,N_A}] \in \mathbb{C}^{N_A \times 1}$. The channel model consisting of distance-dependent large-scale fading and random small-scale fading is considered as

$$\mathbf{h}_{mi} = \beta_{mi}^{\frac{1}{2}} \boldsymbol{\zeta}_{mi}, m \in \omega_B, \quad (1)$$

$$\mathbf{g}_{ji} = \delta_{ji}^{\frac{1}{2}} \boldsymbol{\xi}_{ji}, j \in \omega_A, \quad (2)$$

where β_{mi} and δ_{ji} are path loss of the channel with $\beta_{mi} = \beta_0 d_{mi}^{-\alpha_1}$ and $\delta_{ji} = \delta_0 l_{ji}^{-\alpha_2}$. ω_B and ω_A are the sets of all the BSs and APs, respectively. The small-scale fading in both $\boldsymbol{\zeta}_{mi}$ and $\boldsymbol{\xi}_{ji}$ are independent and identically distributed (i.i.d.) $\mathcal{CN}(0, 1)$ random variables (r.v.s).

The entire network area is represented by \mathcal{A} .

During the downlink transmission, UE in the same cell will be served by the same BS. In addition, both BSs and APs select conjugate beamforming in order to obtain low computational complexity and good performance, and also

to avoid channel state information (CSI) interactions between APs [1]. Therefore, the signal transmitted by BS m is

$$\mathbf{x}_{B,m} = \sqrt{P_B \eta_B} \sum_{n \in \phi_{B,m}} \frac{\mathbf{h}_{mn}}{\|\mathbf{h}_{mn}\|} q_n, \quad (3)$$

where $\phi_{B,m}$ denotes the set of UE that are served by BS m , and $q_n \sim \mathcal{CN}(0, 1)$ denotes the information-bearing symbols for UE n . η_B denotes the power constraint parameter with $\mathbb{E}[\mathbf{x}_{B,m}^H \mathbf{x}_{B,m}] = P_B$. For convenience, η_B is expressed as the average number of users per BS, i.e., $\eta_B = \frac{1}{|\phi_B|} = \frac{\lambda_U}{\lambda_B}$, where $|\phi_B|$ denotes the average of $|\phi_{B,m}|$ for any m .

Denote the set of UE in the network as ϕ_U . Therefore, the corresponding downlink signal from each cell-free AP j is

$$\mathbf{x}_{A,j} = \sqrt{P_A \eta_A} \sum_{i \in \phi_U} \frac{\mathbf{g}_{ji}}{\|\mathbf{g}_{ji}\|} q_i, \quad (4)$$

where η_A denotes the power constraint parameter. Note that the averaged number of UE in ϕ_U is $\mathbb{E}[|\phi_U|] = \bar{U} = \lambda_U |\mathcal{A}|$, η_A can be denoted as $\eta_A = \frac{1}{\bar{U}}$ to ensure $\mathbb{E}[\mathbf{x}_{A,j}^H \mathbf{x}_{A,j}] = P_A$.

For any UE i in the network, i^* is denoted as the index of the associated and nearest BS providing the service. With the collaboration of cell-free APs and cellular BSs, the downlink signal received by the typical UE 0 is

$$\begin{aligned} y_0 &= \sum_{m \in \omega_B} \mathbf{h}_{m0}^H \mathbf{x}_{B,m} + \sum_{j \in \omega_A} \mathbf{g}_{j0}^H \mathbf{x}_{A,j} + n_0 \\ &= \underbrace{\sqrt{P_B \eta_B} \|\mathbf{h}_{00}\|}_{S_{0B}} q_0 + \underbrace{\sum_{j \in \omega_A} \sqrt{P_A \eta_A} \|\mathbf{g}_{j0}\|}_{S_{0A}} q_0 + \\ &\quad \underbrace{\sum_{i \in \phi_U \setminus \{0\}} \left(\sqrt{P_B \eta_B} \mathbf{h}_{i^*0}^H \frac{\mathbf{h}_{i^*i}}{\|\mathbf{h}_{i^*i}\|} + \sqrt{P_A \eta_A} \sum_{j \in \omega_A} \mathbf{g}_{j0}^H \frac{\mathbf{g}_{ji}}{\|\mathbf{g}_{ji}\|} \right)}_{I_U} q_i + n_0, \end{aligned} \quad (5)$$

where the first term S_{0A} and the second term S_{0B} represent the desired signals from BS 0 and cell-free APs, respectively. The total interference is shown in the third term I_U . Each term in I_U consists of the signal sent by cellular BSs and cell-free APs to any other UE. The last term n_0 denotes the additive white Gaussian noise (AWGN) with power σ^2 .

Based on (5), the interference power caused by the signal intended to UE i is given by

$$I_i = \left| \sqrt{P_B \eta_B} \mathbf{h}_{i^*0}^H \frac{\mathbf{h}_{i^*i}}{\|\mathbf{h}_{i^*i}\|} + \sqrt{P_A \eta_A} \sum_{j \in \omega_A} \mathbf{g}_{j0}^H \frac{\mathbf{g}_{ji}}{\|\mathbf{g}_{ji}\|} \right|^2. \quad (6)$$

In interference I_i , BS channel vector \mathbf{h}_{i^*0} is independent of channel vector $\mathbf{g}_{j0}, \forall j \in \omega_A$. Meanwhile, the channel gains \mathbf{g}_{i0} and \mathbf{g}_{j0} from different APs are also independent of each other, $\forall i \neq j$. Taking into account the law of large number and the mutual independence of channels as well as beamforming vectors between different BSs and APs, I_i can be approximated as

$$I_i \approx P_B \eta_B \left| \mathbf{h}_{i^*0}^H \frac{\mathbf{h}_{i^*i}}{\|\mathbf{h}_{i^*i}\|} \right|^2 + P_A \eta_A \sum_{j \in \omega_A} \left| \mathbf{g}_{j0}^H \frac{\mathbf{g}_{ji}}{\|\mathbf{g}_{ji}\|} \right|^2. \quad (7)$$

The approximation in (7) indicates that I_i can be expressed in the form of the sum of the power of the signal from the associated BS i^* and each AP. Further, by classifying the interference into intra-cell interference I_{B0} , inter-cell interference I_B , and interference I_A due to the APs, the total interference $\sum_{i \in \phi_U \setminus \{0\}} I_i$ can be rewritten as

$$\sum_{i \in \phi_U \setminus \{0\}} I_i = I_{B0} + I_B + I_A, \quad (8)$$

where

$$\begin{aligned} I_{B0} &= P_B \eta_B \sum_{n \in \phi_{B,0} \setminus \{0\}} \left| \mathbf{h}_{00}^H \frac{\mathbf{h}_{0n}}{\|\mathbf{h}_{0n}\|} \right|^2, \\ I_B &= P_B \eta_B \sum_{m \in \omega_B \setminus \{0\}} \sum_{n \in \phi_{B,m}} \left| \mathbf{h}_{m0}^H \frac{\mathbf{h}_{mn}}{\|\mathbf{h}_{mn}\|} \right|^2, \\ I_A &= P_A \eta_A \sum_{i \in \phi_U \setminus \{0\}} \sum_{j \in \omega_A} \left| \mathbf{g}_{j0}^H \frac{\mathbf{g}_{ji}}{\|\mathbf{g}_{ji}\|} \right|^2. \end{aligned} \quad (9)$$

Therefore, the corresponding received SINR at UE 0 is approximately expressed as

$$\Omega = \frac{S_0}{I_{B0} + I_B + I_A + \sigma^2}, \quad (10)$$

where

$$S_0 = (S_{0B} + S_{0A})^2 = \left(\sqrt{P_B \eta_B} \|\mathbf{h}_{00}\| + \sqrt{P_A \eta_A} \sum_{j \in \omega_A} \|\mathbf{g}_{j0}\| \right)^2. \quad (11)$$

III. ANALYSIS OF SIGNAL STRENGTH AND INTERFERENCE

In this section, the statistical distributions of the received signal and interference power are characterized. The signal strength is approximated via moment matching, with its first- and second-order moments derived in closed-form. The intra- and inter-cell interference caused by BSs are approximated as a Gamma r.v. and a weighted sum of Gamma r.v.s, respectively. The average interference caused by cell-free APs is derived in closed-form. In addition, the performance of the network can be obtained by analyzing a typical UE 0 according to Slivnyak's theorem [11].

A. Analysis of Channel Distribution

Based on the channel model of BSs and APs, the power of the channel to UE i for the m th BS and the j th AP can be respectively given by

$$|\mathbf{h}_{mi}|^2 = \beta_{mi} \boldsymbol{\zeta}_{mi}^H \boldsymbol{\zeta}_{mi}, \quad (12)$$

$$|\mathbf{g}_{ji}|^2 = \delta_{ji} \boldsymbol{\xi}_{ji}^H \boldsymbol{\xi}_{ji}. \quad (13)$$

Since all the entries in both $\boldsymbol{\zeta}_{mi}$ and $\boldsymbol{\xi}_{ji}$ follow the i.i.d. $\mathcal{CN}(0, 1)$, $\boldsymbol{\zeta}_{mi}$ and $\boldsymbol{\xi}_{ji}$ are isotropic vectors in N_B and N_A dimensions respectively [12].

Note that for the isotropic vector $\mathbf{x} \in \mathbb{C}^{N \times 1}$ with each entry following i.i.d. $\mathcal{CN}(1, \delta^2)$, $\mathbf{x}^H \mathbf{x}$ is the sum of i.i.d. variables $\Gamma(1, \delta^2)$, and thus follows $\Gamma(N, \delta^2)$ [13]. Therefore, we have $\boldsymbol{\zeta}_{00}^H \boldsymbol{\zeta}_{00} \sim \Gamma(N_B, 1)$ and $\boldsymbol{\xi}_{j0}^H \boldsymbol{\xi}_{j0} \sim \Gamma(N_A, 1)$.

Lemma 1. For the Gamma distributed r.v. $X \sim \Gamma(a, \theta)$ and any $b > 0$, $Y = bX \sim \Gamma(a, b\theta)$ [14].

Based on Lemma 1, the BS and AP channel power in (12) and (13) are distributed according to

$$|\mathbf{h}_{mi}|^2 \sim \Gamma(N_B, \beta_{mi}), \quad (14)$$

$$|\mathbf{g}_{ji}|^2 \sim \Gamma(N_A, \delta_{ji}), \quad (15)$$

B. Approximation of the Signal Power Distribution

According to (14), the power of the nearest associated BS channel $|\mathbf{h}_{00}|^2$ is the sum of N_B i.i.d. variables following $\Gamma(1, \beta_{00})$, i.e., $|\mathbf{h}_{00}|^2 \sim \Gamma(N_B, \beta_{00})$. For further analysis of the desired signal S_0 in (9), Lemma 2 about the square root of Gamma variable is first introduced.

Lemma 2. For any Gamma distributed r.v. $X \sim \Gamma(k, \theta)$, the square root Y of X follows the Nakagami distribution as $Y = \sqrt{X} \sim \text{Nakagami}(m, \omega)$ [15], where the parameters are $m = k, \omega = m\theta$.

Therefore, the distribution of $\|\mathbf{h}_{00}\|$ is obtained according to Lemma 2 as

$$\|\mathbf{h}_{00}\| = \sqrt{|\mathbf{h}_{00}|^2} \sim \text{Nakagami}(N_B, N_B \beta_{00}), \quad (16)$$

while the component of AP channel $\|\mathbf{g}_{j0}\|$ in S_0 has

$$\|\mathbf{g}_{j0}\| = \sqrt{|\mathbf{g}_{j0}|^2} \sim \text{Nakagami}(N_A, N_A \delta_{j0}), \forall j \in \omega_A. \quad (17)$$

The distribution of the desired signal S_0 is composed of the signals from the associated BS 0 together with all APs. Considering the random distribution of the cell-free APs in the network, the following Lemma 3 is introduced.

Lemma 3. With the law of large number, the desired signal in S_0 due to the APs can be approximated by their average L_A when the number of APs is large and $\alpha_2 < 4$, i.e.,

$$\begin{aligned} \sqrt{P_A \eta_A} \sum_{j \in \omega_A} \|\mathbf{g}_{j0}\| &\approx \sqrt{P_A \eta_A} \mathbb{E} \left[\sum_{j \in \omega_A} \|\mathbf{g}_{j0}\| \right] \\ &= \underbrace{\frac{4\pi \sqrt{\rho_A} \lambda_A \delta_0^{\frac{1}{2}} \Gamma(N_A + \frac{1}{2})}{4 - \alpha_2} \left(\frac{|A|}{\pi} \right)^{1 - \frac{\alpha_2}{4}}}_{L_A}, \end{aligned} \quad (18)$$

where $\rho_A = P_A \eta_A$. The detailed derivation is based on the Campbell Theorem [11], and will be shown in an extended journal version.

From Lemma 3, the power expression S_0 for the desired signal is simplified as the square of the sum of a Nakagami r.v. and the constant L_A as $S_0 \approx (\sqrt{P_B \eta_B} \|\mathbf{h}_{00}\| + L_A)^2$. Therefore, the following Lemma is introduced.

Lemma 4. For any Nakagami r.v. $X \sim \text{Nakagami}(m, \omega)$, the probability density function (PDF) of the square of the shifted Nakagami r.v. $Y = (X + A)^2$ for $Y > A^2$ is

$$f_Y(y) = \frac{m^m}{\Gamma(m) \omega^m} (\sqrt{y} - A)^{2m-1} \exp\left(-\frac{m}{\omega} (\sqrt{y} - A)^2\right) y^{\frac{1}{2}}. \quad (19)$$

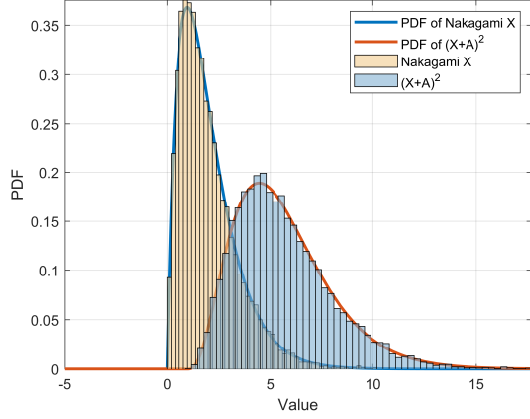


Fig. 2. The distribution of the square of shifted Nakagami r.v. $Y = (X+A)^2$.

The verification of the distribution of $Y = (X+A)^2$ is shown in Fig. 2. From (19) and Fig. 2, the exact distribution of S_0 is difficult to characterize, but the corresponding PDF of S_0 has a similar structure to that of the Gamma distribution. Therefore, with given distance of the nearest associated BS 0, S_0 can be approximated as a Gamma r.v. based on its first- and second-order moments [16]. The corresponding Lemma (5) is introduced as follows.

Lemma 5. According to the definition of the Gamma r.v. [17], the desired signal power S_0 can be approximated as the Gamma distribution $\Gamma(k_{S_0}, \theta_{S_0})$ with

$$\begin{aligned} k_{S_0} &= \frac{(\mathbb{E}\{S_0\})^2}{\text{Var}\{S_0\}} = \frac{(\mathbb{E}\{S_0\})^2}{\mathbb{E}\{S_0^2\} - (\mathbb{E}\{S_0\})^2}, \\ \theta_{S_0} &= \frac{\text{Var}\{S_0\}}{\mathbb{E}\{S_0\}} = \frac{\mathbb{E}\{S_0^2\} - (\mathbb{E}\{S_0\})^2}{\mathbb{E}\{S_0\}}, \end{aligned} \quad (20)$$

where the first- and second-order moments of S_0 are

$$\mathbb{E}\{S_0\} = \rho_B N_B \beta_{00} + 2\rho_B^{\frac{1}{2}} L_A \frac{\Gamma(N_B + \frac{1}{2})}{\Gamma(N_B)} \beta_{00}^{\frac{1}{2}} + L_A^2, \quad (21)$$

$$\begin{aligned} \mathbb{E}\{S_0^2\} &= \rho_B^2 N_B (N_B + 1) \beta_{00}^2 + 4\rho_B^{\frac{3}{2}} L_A \frac{\Gamma(N_B + \frac{3}{2})}{\Gamma(N_B)} \beta_{00}^{\frac{3}{2}} \\ &+ 6\rho_B L_A^2 N_B \beta_{00} + 4\rho_B^{\frac{1}{2}} L_A^3 \frac{\Gamma(N_B + \frac{1}{2})}{\Gamma(N_B)} \beta_{00}^{\frac{1}{2}} + L_A^4. \end{aligned} \quad (22)$$

The detailed derivation is based on the raw moments of Gamma distribution, and is omitted here for space.

C. Analysis of Interference Power Distribution

Similar to the case of the desired signal, the power distribution of the interference is analyzed in this subsection. Considering that conjugate beamforming is applied by both BSs and APs in the network, the Lemma 6 for the projection of isotropic channel vectors is introduced.

Lemma 6. Denote $\mathbf{x} \in \mathbb{C}^{N \times 1}$ as an isotropic vector with i.i.d. $\mathcal{CN}(0, \theta)$ entries. If \mathbf{x} is projected onto an s -dimensional beamforming subspace, the power distribution is [18]

$$|\mathbf{x}^H \mathbf{w}|^2 \sim \Gamma(s, \theta). \quad (23)$$

Based on Lemma 6, the power I_{B0} of intra-cell interference in (9) can be approximated as the sum of $(|\bar{\phi}_B| - 1)$ i.i.d. variables following $\Gamma(1, P_B \eta_B \beta_{00})$. Further, extracting the scale parameter, the power of intra-cell interference can be rewritten as $I_{B0} = P_B \eta_B \beta_{00} \kappa_{B,0}$, where $\kappa_{B,0} \sim \Gamma(|\bar{\phi}_B| - 1, 1)$.

For the inter-cell interference, since \mathbf{h}_{m0} is also independent of \mathbf{h}_{mn} , the interference power of each BS $m \in \omega_B \setminus \{0\}$ in I_B is approximated as $\sum_{n \in \phi_{B,m}} \left| \mathbf{h}_{m0}^H \frac{\mathbf{h}_{mn}}{\|\mathbf{h}_{mn}\|} \right|^2 \sim \Gamma(|\bar{\phi}_B|, \beta_{m0})$. Therefore, as the sum of interference from BSs in $\omega_B \setminus \{0\}$, the inter-cell interference I_B can be further expressed as the sum of Gamma variables with the same shape parameters and scale parameters, i.e.,

$$I_B = P_B \eta_B \sum_{m \in \omega_B \setminus \{0\}} \beta_{m0} \kappa_{B,m0}, \quad (24)$$

where $\kappa_{B,m0} \in \Gamma(|\bar{\phi}_B|, 1), \forall m \in \omega_B \setminus \{0\}$.

Next, we need to analyze the interference I_A from the APs. According to (3) and (6), the following Lemma about I_A is introduced.

Lemma 7. By the law of large number, the interference I_A due to the APs is approximated by its average \bar{I}_A when the number of APs is large and $\alpha_2 < 2$, i.e.,

$$\begin{aligned} I_A &\approx P_A \eta_A \mathbb{E} \left[\sum_{i \in \phi_U \setminus \{0\}} \sum_{j \in \omega_A} \left| \mathbf{g}_{j0}^H \frac{\mathbf{g}_{ji}}{\|\mathbf{g}_{ji}\|} \right|^2 \right] \\ &= \underbrace{\frac{2\pi \rho_A \lambda_A \delta_0 (\lambda_U |\mathcal{A}| - 1)}{2 - \alpha_2}}_{\bar{I}_A} \left(\frac{|\mathcal{A}|}{\pi} \right)^{1 - \frac{\alpha_2}{2}}. \end{aligned} \quad (25)$$

The detailed derivation is based on the Campbell Theorem [11], and will be shown in an extended journal version.

IV. COVERAGE PROBABILITY OF HYBRID CELLULAR AND CELL-FREE NETWORK

In this section, the coverage probability of hybrid cellular and cell-free network is analyzed based on the distribution of signal strength and various interference components, derived in the preceding section. In general, the coverage probability is the complementary cumulative distribution function (CCDF) of SINR over the overall network, which can be defined as

$$p_c \triangleq \mathbb{P}[\Omega = \frac{S_0}{I_{B0} + I_B + \bar{I}_A + \sigma^2} > T], \quad (26)$$

where T denotes the target threshold of the SINR Ω .

A. Analysis of Coverage Probability

Taking the distance d_{00} between the typical UE 0 and its associated and nearest BS 0 as an r.v., the average coverage probability in the network is

$$p_c = \mathbb{E}[p_c(d_{00})] = \int_0^{\sqrt{\frac{|\mathcal{A}|}{\pi}}} p_c(r) f_{d_{00}}(r) dr, \quad (27)$$

where $f_{d_{00}}(r)$ denotes the PDF of the nearest point distance in PPP. With the cumulative distribution function (CDF) of r.v. d_{00} as $F_{d_{00}}(r) = 1 - e^{-\lambda_B \pi r^2}$ [11], there is

$$f_{d_{00}}(r) = \frac{dF_{d_{00}}(r)}{dr} = 2\lambda_B \pi r e^{-\lambda_B \pi r^2}. \quad (28)$$

First, the relationship between intra-cell interference I_{B0} and inter-cell interference I_B is analyzed. Clearly, both I_{B0} and I_B are dependent on the distance d_{00} , i.e., I_{B0} comes from the associated BS 0 with a distance of d_{00} , and I_B comes from the other BSs with distances $d \geq d_{00}$. However, there is no interaction between I_{B0} and I_B . Specifically, with the given d_{00} , I_{B0} depends on the distribution of UE in the cell of BS 0, while I_B depends mainly on the distribution of other BSs with a distance no smaller than d_{00} . Therefore, I_{B0} and I_B are independent of each other with a given d_{00} . Therefore, the coverage probability can be further expressed as in Lemma 8.

Lemma 8. Considering that the desired signal S_0 following the Gamma distribution, i.e., $S_0 \sim \Gamma(k_{S_0}, \theta_{S_0})$ the network coverage probability in (26) can be expressed as

$$p_c(d_{00}) = \mathbb{P}[S_0 > T(I_{B0} + I_B + \bar{I}_A + \sigma^2)] \\ = \sum_{i=0}^{k_{S_0}-1} \frac{(-1)^i}{i!} \frac{\partial^i}{\partial^i s} \left\{ e^{-s \frac{TI_e}{\theta_{S_0}}} \mathcal{L}_{Y_{I_{B0}}}(s) \mathcal{L}_{Y_{I_B}}(s) \right\}_{s=1}, \quad (29)$$

where the sum of interference from APs and noise is denoted as $I_e = \bar{I}_A + \sigma^2$. The shape parameter k_{S_0} is integer. The Laplace transforms of $Y_{I_{B0}} = \frac{TI_{B0}}{\theta_{S_0}}$ and $Y_{I_B} = \frac{TI_B}{\theta_{S_0}}$ are

$$\mathcal{L}_{Y_{I_{B0}}}(s) = \left(1 + s \frac{T\rho_B \beta_0 d_{00}^{-\alpha_1}}{\theta_{S_0}}\right)^{1-|\bar{\phi}_B|}, \\ \mathcal{L}_{Y_{I_B}}(s) = \exp\left(2\pi\lambda_B \int_{d_{00}}^{\sqrt{\frac{|A|}{\pi}}} \left[(1 + s \frac{T\rho_B \beta_0 r^{-\alpha_1}}{\theta_{S_0}})^{-|\bar{\phi}_B|} - 1\right] r dr\right). \quad (30)$$

Based on Lemma 8, the analysis of the coverage probability is transformed into the analysis of the higher-order derivatives, and the coverage of probability is rewritten as

$$p_c(d_{00}) = \sum_{i=0}^{k_{S_0}-1} \frac{(-1)^i}{i!} \frac{\partial^i}{\partial^i s} \left\{ L(s) \right\}_{s=1}, \quad (31)$$

where

$$L(s) = e^{-s \frac{TI_e}{\theta_{S_0}}} \cdot \left(1 + s \frac{T\rho_B \beta_0 d_{00}^{-\alpha_1}}{\theta_{S_0}}\right)^{1-|\bar{\phi}_B|} \\ \cdot \exp\left(2\pi\lambda_B \int_{d_{00}}^{\sqrt{\frac{|A|}{\pi}}} \left[(1 + s \frac{T\rho_B \beta_0 r^{-\alpha_1}}{\theta_{S_0}})^{-|\bar{\phi}_B|} - 1\right] r dr\right). \quad (32)$$

The higher-order derivatives of $L(s)$ is derived in the next part.

B. Evaluation of Higher-order Derivatives

The objective function $L(s)$ of the higher-order derivatives in (31) is rewritten in the form of the exponential function, i.e.,

$$L(s) = \exp\left\{ \underbrace{-s \frac{TI_e}{\theta_{S_0}}}_{D_1(s)} + \underbrace{(1 - |\bar{\phi}_B|) \ln\left(1 + s T \theta_{S_0} d_{00}^{-\alpha_1}\right)}_{D_2(s)} \right. \\ \left. + \underbrace{2\pi\lambda_B \int_{d_{00}}^{\sqrt{\frac{|A|}{\pi}}} \left[(1 + s T \theta_{S_0} r^{-\alpha_1})^{-|\bar{\phi}_B|} - 1\right] r dr}_{D_3(s)} \right\}, \quad (33)$$

where $T \theta_{S_0} = \frac{T\rho_B \beta_0}{\theta_{S_0}}$ is applied for convenience.

Since $L(s)$ is a composite function of $g(s) = D_1(s) + D_2(s) + D_3(s)$, the special case of Faà di Bruno's formula with exponential functions can be applied to efficiently derive the i th order derivatives of $L(s)$ [16], [19], i.e.,

$$\frac{\partial^i}{\partial^i s} L(s) = \frac{\partial^i}{\partial^i s} \left\{ \exp(g(s)) \right\} = \exp(g(s)) B_i\left(\frac{\partial^1 g(s)}{\partial^1 s}, \dots, \frac{\partial^i g(s)}{\partial^i s}\right), \quad (34)$$

where $B_i(x_1, \dots, x_i)$ denotes the i th complete exponential Bell polynomial, whose coefficients can be efficiently obtained according to its definition [20], [21]. The remaining work is to evaluate the higher-order derivatives of $g(s)$, which can be decomposed as

$$\frac{\partial^i g(s)}{\partial^i s} = \frac{\partial^i D_1(s)}{\partial^i s} + \frac{\partial^i D_2(s)}{\partial^i s} + \frac{\partial^i D_3(s)}{\partial^i s}. \quad (35)$$

For $D_1(s)$, the derivatives from order 1 to order $(k_{S_0} - 1)$ can be expressed respectively as

$$\frac{\partial^i D_1(s)}{\partial^i s} = \begin{cases} -\frac{TI_e}{\theta_{S_0}}, & i = 1 \\ 0, & i > 1 \end{cases} \quad (36)$$

Additionally, for $D_2(s)$, there is

$$\frac{\partial^i D_2(s)}{\partial^i s} = (-1)^{i-1} (1 - |\bar{\phi}_B|) (i-1)! \left(\frac{T \theta_{S_0} d_{00}^{-\alpha_1}}{1 + T \theta_{S_0} d_{00}^{-\alpha_1} s} \right)^i. \quad (37)$$

Finally, the higher-order derivatives of $D_3(s)$ is

$$\frac{\partial^i D_3(s)}{\partial^i s} = \\ 2\pi\lambda_B \int_{d_{00}}^{\sqrt{\frac{|A|}{\pi}}} \frac{(|\bar{\phi}_B| + i - 1)!}{(|\bar{\phi}_B| - 1)!} \cdot \frac{(-T \theta_{S_0} r^{-\alpha_1})^i}{(1 + T \theta_{S_0} r^{-\alpha_1} s)^{|\bar{\phi}_B| + i}} r dr. \quad (38)$$

Finally, the network coverage probability can be obtained by substituting (31) with (36), (37) and (38) back into (27).

V. SIMULATION RESULTS

In this section, the analytical results of the coverage probability of the hybrid cell and cell-free network are verified by the comparison with the Monte-Carlo (MC) simulation results. Each result of the MS simulation is averaged from 1000 randomly generated wireless node distributions with 5

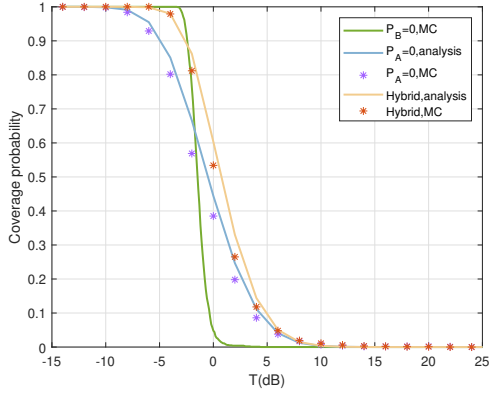


Fig. 3. Coverage probability of different architectures under different T .

realizations per channel. All the wireless nodes are randomly distributed in a circular area of radius 500m and UE 0 is located at the center of the circle. The densities of BSs, APs and UE are $\lambda_B = 40/\text{km}^2$, $\lambda_A = 200/\text{km}^2$ and $\lambda_U = 160/\text{km}^2$, respectively. Other relevant parameters are as follows: $\alpha_1 = 2.7$, $\alpha_2 = 1.8$, $\frac{P_B}{\sigma^2} = 130\text{dB}$, $P_A = 3 \times 10^{-5}P_B$, $N_B = 4$, $N_A = 2$, $C = 3 \times 10^8\text{m/s}$, $f = 3.5\text{GHz}$ and $\beta_0 = \delta_0 = (\frac{C}{4\pi f})^2$.

Fig. 3 shows the coverage probability in cellular networks ($P_A = 0$), cell-free networks ($P_B = 0$), and hybrid cellular and cell-free networks for different SINR thresholds T . The coverage probability is obtained from the linear weighted probability of the upper and lower integers of k_{θ_S} , i.e.,

$$p_c = (\lceil k_{\theta_S} \rceil - k_{\theta_S})p_{c, \lfloor k_{\theta_S} \rfloor} + (k_{\theta_S} - \lfloor k_{\theta_S} \rfloor)p_{c, \lceil k_{\theta_S} \rceil}. \quad (39)$$

From Fig. 3, It is expected that the coverage probability analysis of the hybrid network is generally consistent with the results of the MC simulation under different SINR threshold, and can also be applied to the special case where $P_A = 0$. Compared with traditional cellular networks, hybrid networks effectively improve the communication performance of edge UE and reduce the performance gaps between UE. Compared with cell-free networks, such hybrid networks can achieve higher peak SINR. Therefore, by deploying low-power APs, hybrid cellular and cell-free networks can provide UE with uniformly good communication services while obtaining better peak SINR performance.

VI. CONCLUSION

In this paper, the hybrid cellular and cell-free network is modeled by the stochastic geometry approach, revealing the coupling of the signal and interference from both the cellular and cell-free networks. Moment matching is used to approximate the aggregate signal received from the hybrid network to address the difficulty of distribution analysis due to conjugate beamforming. The coverage probability is then obtained by the Laplace transform for interference. The analysis of the coverage probability of hybrid networks is validated by MC simulation, demonstrating that hybrid networks can reduce the performance gap while improving the peak SINR performance.

VII. ACKNOWLEDGMENT

This work was supported by the National Key R&D Program of China with Grant number 2019YFB1803400, and by the National Natural Science Foundation of China with grant number 62071114.

REFERENCES

- [1] H. Q. Ngo, A. Ashikhmin, H. Yang, E. G. Larsson, and T. L. Marzetta, "Cell-free massive MIMO versus small cells," *IEEE Trans. Wirel. Commun.*, vol. 16, no. 3, pp. 1834–1850, Mar. 2017.
- [2] D. Wang, M. Wang, P. Zhu, J. Li, J. Wang, and X. You, "Performance of network-assisted full-duplex for cell-free massive MIMO," *IEEE Trans. Commun.*, vol. 68, no. 3, pp. 1464–1478, Mar. 2020.
- [3] E. Nayebi, A. Ashikhmin, T. L. Marzetta, H. Yang, and B. D. Rao, "Precoding and power optimization in cell-free massive MIMO systems," *IEEE Trans. Wirel. Commun.*, vol. 16, no. 7, pp. 4445–4459, Jul. 2017.
- [4] Z. Dai, J. Xu, Y. Zeng, S. Jin, and T. Jiang, "Characterizing the rate region of active and passive communications with RIS-based cell-free symbiotic radio," *IEEE Internet Things J.*, pp. 1–1, 2023, early access, doi:10.1109/IOT.2023.3308970.
- [5] T. Kim, H. Kim, S. Choi, and D. Hong, "How will cell-free systems be deployed?" *IEEE Commun. Mag.*, vol. 60, no. 4, pp. 46–51, Apr. 2022.
- [6] S. Elhoushy and W. Hamouda, "Towards high data rates in dynamic environments using hybrid cell-free massive MIMO/small-cell system," *IEEE Wireless Commun. Lett.*, vol. 10, no. 2, pp. 201–205, Feb. 2021.
- [7] A. Papazafeiropoulos, P. Kourtessis, M. D. Renzo, S. Chatzinotas, and J. M. Senior, "Performance analysis of cell-free massive MIMO systems: A stochastic geometry approach," *IEEE Trans. Veh. Technol.*, vol. 69, no. 4, pp. 3523–3537, Apr. 2020.
- [8] T. M. Hoang, H. Q. Ngo, T. Q. Duong, H. D. Tuan, and A. Marshall, "Cell-free massive MIMO networks: Optimal power control against active eavesdropping," *IEEE Trans. Commun.*, vol. 66, no. 10, pp. 4724–4737, Oct. 2018.
- [9] Z. Chen and E. Björnson, "Channel hardening and favorable propagation in cell-free massive MIMO with stochastic geometry," *IEEE Trans. Commun.*, vol. 66, no. 11, pp. 5205–5219, Nov. 2018.
- [10] Y. J. Chun, M. O. Hasna, and A. Ghayeb, "Modeling heterogeneous cellular networks interference using poisson cluster processes," *IEEE J. Sel. Areas Commun.*, vol. 33, no. 10, pp. 2182–2195, Oct. 2015.
- [11] J. G. Andrews, F. Baccelli, and R. K. Ganti, "A tractable approach to coverage and rate in cellular networks," *IEEE Trans. Commun.*, vol. 59, no. 11, pp. 3122–3134, Nov. 2011.
- [12] "Isotropic vectors," http://encyclopediaofmath.org/index.php?title=Isotropic_vector&oldid=54444, Encyclopedia of Mathematics.
- [13] R. W. Heath Jr, T. Wu, Y. H. Kwon, and A. C. K. Soong, "Multiuser MIMO in distributed antenna systems with out-of-cell interference," *IEEE Trans. Signal Process.*, vol. 59, no. 10, pp. 4885–4899, Oct. 2011.
- [14] P. G. Moschopoulos, "The distribution of the sum of independent gamma random variables," *Ann. Inst. Stat. Math.*, vol. 37, no. 1, pp. 541–544, 1985.
- [15] L.-F. Huang, "The nakagami and its related distributions," *WSEAS Trans. Math.*, vol. 15, no. 44, pp. 477–485, 2016.
- [16] J. Lyu and R. Zhang, "Hybrid active/passive wireless network aided by intelligent reflecting surface: System modeling and performance analysis," *IEEE Trans. Wirel. Commun.*, vol. 20, no. 11, pp. 7196–7212, Nov. 2021.
- [17] H. Pishro-Nik, *Introduction to probability, statistics, and random processes*. Kappa Research, LLC Blue Bell, PA, USA, 2014.
- [18] R. J. Muirhead, *Aspects of Multivariate Statistical Theory*. Wiley Series in Probability and Statistics. New York, NY, USA: Wiley, 1982., 1982.
- [19] W. P. Johnson, "The curious history of Faà di Bruno's formula," *Amer. Math. Monthly*, vol. 109, no. 3, pp. 217–234, 2002. [Online]. Available: <http://www.maa.org/news/monthly217-234.pdf>
- [20] R. Tanbourgi, H. S. Dhillon, J. G. Andrews, and F. K. Jondral, "Dual-branch MRC receivers under spatial interference correlation and nakagami fading," *IEEE Trans. Commun.*, vol. 62, no. 6, pp. 1830–1844, Jun. 2014.
- [21] V. F. Ivanoff, "Problems for solution: 4782," *Amer. Math. Monthly*, vol. 65, no. 3, p. 212, 1958. [Online]. Available: <http://www.jstor.org/stable/2310076>.